CHAPTER 3

DESIGN AND SIMULATION OF THE SENSOR

In this chapter, the design of piezoresistive pressure and tactile sensors based on a circular membrane with center boss structure is described respectively. According to the geometry of the sensor, the analytic solutions are developed in order to determine the sensitivity of the sensor. Then, some guidelines to design highly sensitive piezoresistive sensors are suggested from these derived equations. Finally, FEM (Finite Element Method) is used to verify the derived solutions.

3.1 Design of Piezoresistive Pressure Sensors Based on Circular Membrane with Center Boss Structure

3.1.1 Introduction

For regular silicon piezoresistive pressure sensors, p-type single crystal piezoresistors are used and placed at the edge of a rectangular membrane because their longitudinal piezoresistive effect is comparable with their transverse one but with an opposite numerical sign. Therefore, a Wheatstone bridge with differential signal can be realized, which can maximize the sensitivity of the sensor. However, poly-Si and 6H-SiC have a longitudinal piezoresistive effect that is much larger than its transverse one. With such sensing elements, a structure which can provide longitudinal stresses with different numerical signs is required if a half or full Wheatstone bridge is to be used for the measurements. Conventionally, a mechanical structure with a circular membrane and an inner circular center boss provides such a function. It is known that this kind of sensors has longitudinal stresses with different signs at the outer edge and inner edge of the membrane when a pressure is applied to the membrane. Such a structure was first used in the micro silicon pressure sensor by Shimazoe and his co-workers[33]. They showed that a silicon diaphragm with a center boss could solve the problem of large pressure-induced deflection of the diaphragm, which occurs when using membranes without center boss. Then, Schäfer[9] and Yasukawa[34] used the same structure to fabricate pressure sensors with polysilicon piezoresistors and diffused silicon piezoresistors, respectively. Recently, the pressure sensor with a circular center boss was widely used in Microsensor and Actuator Technology Center at TU-Berlin[18][35-37] because it provides high sensitivity and over-range protection after the center boss touches the bottom plate. In contrast with its well-known applications, the analytic solution and the working principle of such kind of sensors have not been discussed in detail. Therefore, a hand-calculation prior to the FEM simulation is not possible. In this section, the analytic solution of this kind of sensors will be derived in order to obtain the design concept.

3.1.2 Analysis

The center boss pressure sensors (CBPS) based on silicon was analyzed by Yasukawa[34] using the beam theory. Here, we start from the plate theory[38] and consider only the effect of small deflections. As illustrated in Fig. 3.1, three working conditions of a CBPS are considered: (a) the outer edge of the membrane is fixed while the center boss is free, (b) the outer edge of the membrane and the center boss are fixed and (c) the outer edge of the membrane is fixed and the center boss has a distance from the bottom plate. This will be discussed in the following sections.

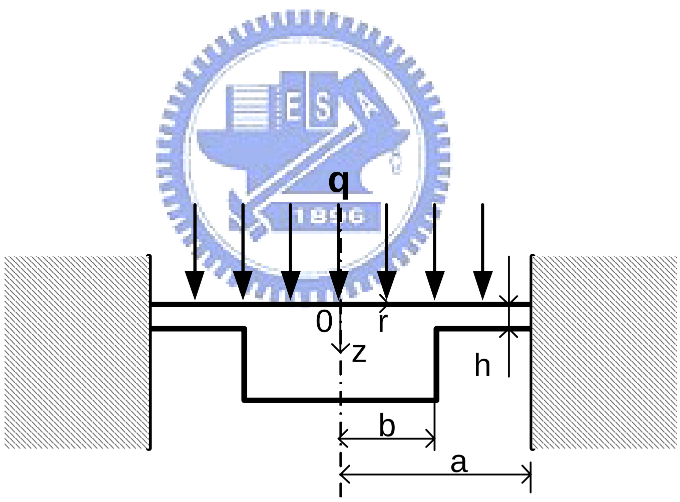

(a)

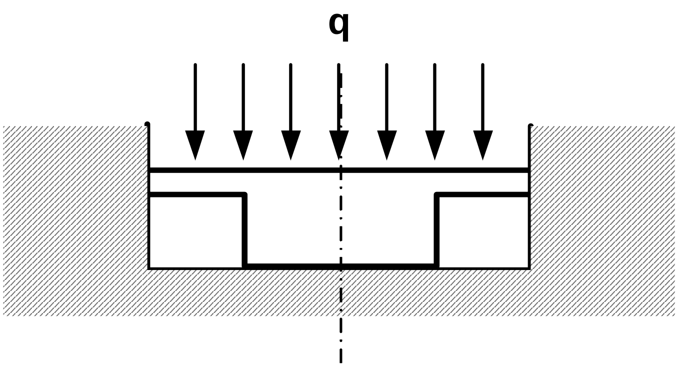

(b)

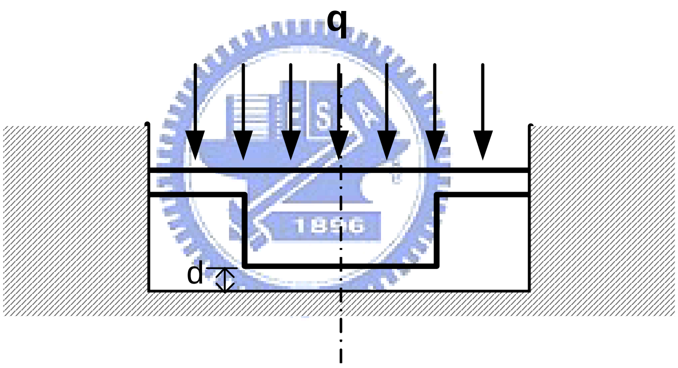

(c)

Figure 3.1. Three working conditions of a center boss pressure sensor: (a) the outer edge of the membrane is fixed and the center boss is free. (b) both the outer edge of the membrane and the center boss are fixed. (c) the outer edge of the membrane is fixed and the center boss has a distance from the bottom.

Case (A) The outer edge of the membrane is fixed while the center boss is free

The general equation of uniformly loaded circular plates can be expressed as follows:

$$\frac{d}{dr}\left[\frac{1}{r}\frac{d}{dr}\left(r\frac{dw_1(r)}{dr}\right)\right]=\frac{qr}{2D} \tag{3.1}$$

where w is the deflection due to the applied intensity load q and r is the radial distance. D is called the flexural rigidity of the plate and is defined as

$$D=\frac{Eh^3}{12(1-\nu^2)} \tag{3.2}$$

where E is the Young's modulus, ν is the Poisson's ratio and h is the thickness of the plate.

The general solution of this differential equation can be represented by

$$w_1(r)=\frac{qr^4}{64D}+\frac{C_1r^2}{4}+C_2\ln\frac{r}{a}+C_3 \tag{3.3}$$

where the three unknown constants, C_1, C_2 and C_3, will be determined by three suitable boundary conditions. For a circular membrane with a center boss, the deflection and the slope of the membrane at the circumference and at the edge of the center boss are zero if the center boss is assumed as a rigid body. So the following boundary conditions are used to find the analytic solution:

$$w_1(a) = 0, \; w_1'(a) = 0 \text{ and } w_1'(b) = 0 \tag{3.4}$$

After solving the differential equation, Eq. (3.1), the deflection of the membrane can be expressed as

$$w_1(r) = \frac{qa^4}{64D}\left[(1-(\frac{r}{a})^2)(1+2(\frac{b}{a})^2-(\frac{r}{a})^2)+4(\frac{b}{a})^2\ln\frac{r}{a}\right], \quad b \le r \le a \tag{3.5}$$

The normalization is made by the substitution of b to na and r to ax, so the above equation can be rewritten as

$$w_1(x) = \frac{qa^4}{64D}\left[(1-x^2)(1+2n^2-x^2)+4n^2\ln x\right], \; 0 \le n < 1, \; n \le x \le 1 \tag{3.6}$$

which agrees to the result by Engl[39]. The correspondent longitudinal and transverse stress at the top surface of the annular membrane where the piezoresistors are placed can be obtained by the following equations,

$$\sigma_{r1}(r) = -\frac{6M_r(r)}{h^2} = \frac{6D}{h^2}\left(\frac{d^2w(r)}{dr^2}+\frac{\nu}{r}\frac{dw(r)}{dr}\right) \tag{3.7}$$

and

$$\sigma_{t1}(r) = -\frac{6M_t(r)}{h^2} = \frac{6D}{h^2}\left(\frac{1}{r}\frac{dw(r)}{dr}+\nu\frac{d^2w(r)}{dr^2}\right). \tag{3.8}$$

Therefore, the longitudinal and transverse stresses, caused by the deflection are

$$\sigma_{r1}(x) = -\frac{3qa^2}{8h^2}[(1-\nu)(\frac{n}{x})^2+(1+\nu)(1+n^2)-(3+\nu)x^2] \tag{3.9}$$

and

$$\sigma_{t1}(x) = -\frac{3qa^2}{8h^2}[-(1-\nu)(\frac{n}{x})^2 + (1+\nu)(1+n^2) - (1+3\nu)x^2], \qquad (3.10)$$

respectively. If $n = 0$ is substituted in Eq. (3.9) and (3.10), which means a circular membrane without a center boss structure, the solutions for the deflection and the longitudinal and transverse stress are coincident to a pressure sensor with a circular membrane that has a radius a

$$w_1(x) = \frac{qa^4}{64D}(1-x^2)^2 \qquad (3.11)$$

$$\sigma_{r1}(x) = -\frac{3qa^2}{8h^2}[(1+\nu) - (3+\nu)x^2] \qquad (3.12)$$

$$\sigma_{t1}(x) = -\frac{3qa^2}{8h^2}[(1+\nu) - (1+3\nu)x^2] \qquad (3.13)$$

From Eqs. (3.9), (3.10), (3.12) and (3.13), we can see that both the stresses of these two structures are proportional to the square of the ratio of the membrane's radius to the membrane's thickness. Table 3.1 summarizes some properties of a circular membrane with and without a center boss. To make a high sensitivity piezoresistive sensor, the piezoresistors are placed at the positions where the maximum values of the longitudinal and transverse stress occur. As we can see from Table 3.1, these positions are at the center ($x = 0$) of the circular membrane pressure sensor (CMPS) and at the inner ($x = n$) and outer ($r = 1$) edge of the CBPS. For a CBPS, the magnitudes of the longitudinal stresses at the inner and outer edge of the annular membrane are the same but have the opposite sign. Therefore, the CBPS needs only the longitudinal stress to form a full Wheatstone bridge.

Table 3.1 Properties of circular membranes with and without center boss structure.

Membrane type / Properties		Circular	Center-Boss
Max. deflection		$w(0)=\frac{qa^4}{64D}$	$w(n)=\frac{qa^4}{64D}(1+4n^2\ln n-n^4)$
Long. Stress	inner	$\sigma_r(0)=-\frac{3qa^2}{8h^2}(1+\nu)$	$\sigma_r(n)=-\frac{3qa^2(1-n^2)}{4h^2}$
	outer	$\sigma_r(1)=\frac{3qa^2}{4h^2}$	$\sigma_r(1)=\frac{3qa^2(1-n^2)}{4h^2}$
Tran. Stress	inner	$\sigma_t(0)=\frac{3qa^2}{8h^2}(1+\nu)$	$\sigma_t(n)=\nu\frac{3qa^2(1-n^2)}{4h^2}$
	outer	$\sigma_t(1)=-\nu\frac{3qa^2}{4h^2}$	$\sigma_t(1)=-\nu\frac{3qa^2(1-n^2)}{4h^2}$

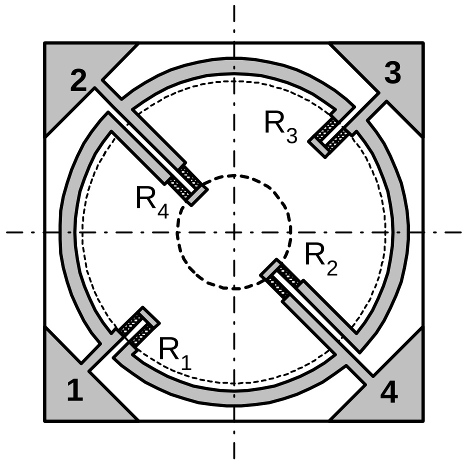

(a)

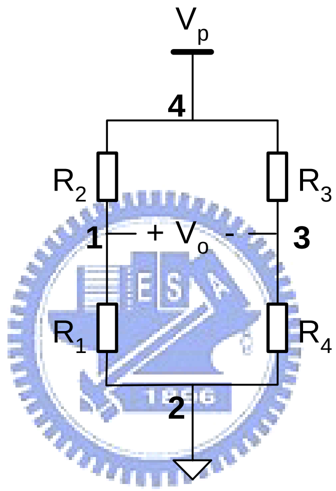

(b)

Figure 3.2. Arrangement of the piezoresistors on the center boss pressure sensor (a) top view of the sensor chip (b) the schematic view of the sensor.

Fig. 3.2 shows the position of the piezoresistors on the CBPS. This schematic will be used to design and calculate the sensitivity of the sensor. The sensitivity of the CBPS is

$$S_1 = \frac{R_1}{R_1 + R_2} - \frac{R_4}{R_3 + R_4} = \frac{\Delta R_o - \Delta R_i}{2R_0} = \pi_r(\sigma_{r1}(1) - \sigma_{r1}(n))/2 = \pi_r \frac{3qa^2(1-n^2)}{4h^2}, \tag{3.14}$$

where R_0 is the piezoresistor's resistance without stress, ΔR_o and ΔR_i are the changes in the resistance at the outer and inner circumference of the annular membrane, respectively. For the CMPS structure, we get

$$S_{1c} = \pi_r \sigma_{r1c}(n) = \pi_r \frac{3qa^2(1+\nu^2)}{8h^2}, \tag{3.15}$$

where $\sigma_{r1c}(n)$ is the longitudinal stress of CMPS at the outer edge of the circular membrane. Comparing Eq. (3.14) and (3.15), we find that the sensitivity of CBPS is two times larger than that of CMPS if a full Wheatstone bridge is used.

Case (B) The outer edge of the membrane and the center boss is fixed

This condition can be modeled by an annular membrane with a built-in inner and outer fixture as illustrated in Fig. 3.3. To solve this problem, the differential equation for a circular membrane with an intensity q of the load distributed over the plate is used and expressed as

$$\frac{1}{r}\frac{d}{dr}\left\{r\frac{d}{dr}\left[\frac{1}{r}\frac{d}{dr}\left(r\frac{dw_2(r)}{dr}\right)\right]\right\} = \frac{q}{D} \tag{3.16}$$

With the following boundary conditions,

$$w_2(a)=0,\ \ w_2(b)=0,\ \ w_2'(a)=0 \text{ and } w_2'(b)=0 \tag{3.17}$$

which are the same conditions as for a clamped-clamped beam, Eq. (3.16) can be solved and normalized as

$$\begin{aligned} w_2(x) \quad = \quad & \frac{qa^4}{64D((1-n^2)^2-4n^2\ln^2 n)}\Big\{\Big[\left(1-n^2\right)^2-4n^2\ln^2 n)\Big]x^4+ \\ & \left[8n^2\ln^2 n-(1-n^2)^2(1+n^2)(1+2\ln x)+2n^2(-1+n^2)(-1+n^2+4\ln x)\ln n\right]x^2 \\ & -n^2\left[4\ln^2 n-(1-n^2)^2(1+4\ln x)+2\ln n((1-n^2)^2+2(-1+n^4)\ln x)\right]\Big\} \end{aligned} \tag{3.18}$$

So the distribution of the longitudinal and transverse stresses can be obtained according to Eq. (3.7) and (3.8),

$$\begin{aligned} \sigma_{r2}(x) \quad = \quad & \frac{3a^2q}{8h^2x^2\left[(1-n^2)^2-4n^2\ln^2 n\right]}\Big\{-4n^2x^2\left[-1+3x^2+\nu(-1+x^2)\right]\ln^2 n \\ & +n^2(-1+n^2)\ln n\left[1-\nu+5x^2+\nu x^2+n^2\left(1+x^2+\nu(-1+x^2)\right)+4(1+\nu)x^2\ln x\right] \\ & -(1-n^2)^2\left[x^2(2+\nu-3x^2-\nu x^2)+n^2\left(1+2x^2+\nu(-1+x^2)\right)+(1+n^2)(1+\nu)x^2\ln x\right]\Big\} \end{aligned} \tag{3.19}$$

and

$$\begin{aligned} \sigma_{t2}(x) \quad = \quad & \frac{3a^2q}{8h^2x^2\left[(1-n^2)^2-4n^2\ln^2 n\right]}\Big\{-4n^2x^2\left[-1+x^2+\nu(-1+3x^2)\right]\ln^2 n+ \\ & n^2(-1+n^2)\ln n\left[-1+\nu+x^2+5\nu x^2+n^2\left(-1+x^2+\nu(1+x^2)\right)+4(1+\nu)x^2\ln x\right] \\ & -(1-n^2)^2\left[n^2(-1+\nu+x^2+2\nu x^2)-x^2\left(-1+x^2+\nu(-2+3x^2)\right)+(1+n^2)(1+\nu)x^2\ln x\right]\Big\} \end{aligned} \tag{3.20}$$

The longitudinal stresses at the outer and inner edges of the membrane are taken into consideration:

$$\sigma_{r2}(1) = \frac{3a^2q}{8h^2}\frac{(1-n^2)^2(1-3n^2)+2n^2(-3+2n^2+n^4-4\ln n)\ln n}{(1-n^2)^2-4n^2\ln^2 n} \tag{3.21}$$

$$\sigma_{r2}(n) = \frac{3a^2q}{8h^2}\frac{(1-n^2)^2(-3+n^2)-2(-3n^4+2n^2+1+4n^4\ln n)\ln n}{(1-n^2)^2-4n^2\ln^2 n} \tag{3.22}$$

If this structure is used as a pressure sensor and the piezoresistors are placed at the outer and inner edge of the membrane as in Case (A), the sensitivity of the sensor is

$$S_2 = \pi_r \frac{3qa^2}{8h^2}\frac{(1-n^2)(2(1-n^2)^2+(1-n^4)\ln n-4n^2\ln^2 n)}{(1-n^2)^2-4n^2\ln^2 n} \tag{3.23}$$

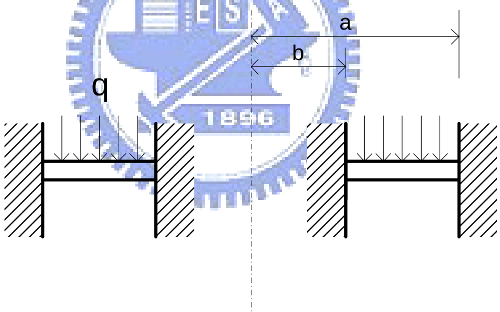

Figure 3.3. Model used to analysis the deflection and stress distribution when both the outer edge of the membrane and the center boss are fixed.

Case (C) The outer edge of the membrane is fixed and the center boss has a distance from the bottom plate

In this case, the center boss of the CBPS will touch the bottom plate when the deflection of the membrane is larger than the distance between the center boss and the bottom plate d. This design is usually adapted for an over-range protection. Before the center boss touches the bottom plate, the solutions of Case (A) can be used. The solutions after the center boss touches the bottom can be obtained by a superposition of the solutions from Case (A) and (B) and expressed as

$$w_3(r) = w_1(r)\big|_{q=q_{th}} + w_2(r)\big|_{q=q-q_{th}} \tag{3.24}$$

$$\sigma_{r3}(r) = \sigma_{r1}(r)\big|_{q=q_{th}} + \sigma_{r2}(r)\big|_{q=q-q_{th}} \tag{3.25}$$

$$\sigma_{t3}(r) = \sigma_{t1}(r)\big|_{q=q_{th}} + \sigma_{t2}(r)\big|_{q=q-q_{th}} \tag{3.26}$$

where the threshold pressure q_{th}, is the pressure when the deflection of the membrane equal to d. q_{th} can be obtained by considering the maximum stress, which is defined as the longitudinal stress at the inner edge, $\sigma_{r1}(n)$, multiplied by a safety factor η, so it doesn't become larger than the yield stress of the material σ_{ys}. From Table 3.1, the following equation can be obtained.

$$q_{th} = \frac{4h^2}{3a^2(1-n^2)}\eta \cdot \sigma_{ys} \tag{3.27}$$

After substituting this equation into Eqs. (3.24), (3.25) and (3.26), the distribution of the deflection and the stresses can be obtained. If Eq. (3.27) is substituted into $w_1(n)$, the maximum allowable deflection of the membrane is

$$d = w_1(n)\big|_{q=q_{th}} = \frac{(1-\nu^2)\eta\sigma_{ys}}{4Eh(1-n^2)}(1+4n^2\ln n - n^4) \tag{3.28}$$

Therefore, the distance between the center boss and the bottom plate can be calculated in order to have an over-range protection for the sensor.

3.1.3 Simulation and Discussion

Numerical figures are calculated and pesented in order to obtain a concrete concept for the distribution of the membrane's deflection and stress under different conditions. The calculation is made, using the following parameters. For a membrane based on (100) silicon, the Youngs' modulus and Poisson's ratio along <001> orientations are 130 GPa and 0.28, respectively[40]. The radius and the thickness of the membrane are 1 mm and 50 μm respectively, which can be achieved by a normal MEMS (Micro Electro-Mechanical System) process. The load for the simulation is a 1 bar pressure.

FEM based on ANSYS® software[41] is used to verify these approximate solutions. An element called SHELL51 is used for the simulation of Case (A) and (B). For the simulation of Case (C), another two elements called TARGE169 and CONTA174 are introduced to perform the simulation after the center boss touches the bottom. The simulated results are illustrated beside the corresponding analytic solution.

First, the distributions of the deflection, longitudinal and transverse stress along the radial distance with respect to different ratios of Case (A) are illustrated in Fig. 3.4.

From this figure, the absolute maximal values of the deflection and the longitudinal and transverse stress occur as n approaches 0, which is a circular membrane. So if only one piezoresistor or a fourth Wheatstone bridge is needed, a circular membrane will yield the maximum output signal since it provides the maximum stress at the same intensity of the loading pressure. However, a full Wheatstone bridge is usually adapted for a pressure sensor because it provides not only the maximum sensitivity but also eliminates the non-differential noise in comparison to the quarter and half bridges. Four piezoresistors with 2 pairs having the same sensitivity but opposite signs must exist in a piezoresistive pressure sensor. Here, the circular membrane would not be a suitable choice. But for a circular membrane with a center boss, the same longitudinal stress with opposite signs can be found at the inner and outer edge of the circular membrane, thus it has a larger sensitivity than a circular membrane if a full Wheatstone bridge is used.

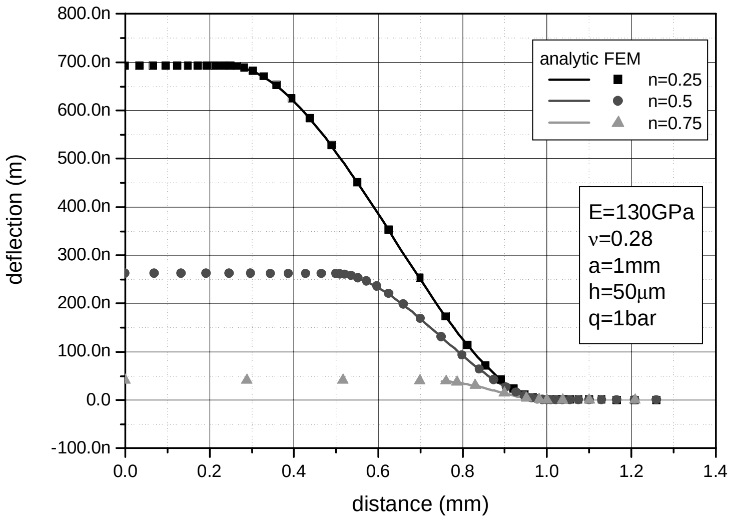

(a)

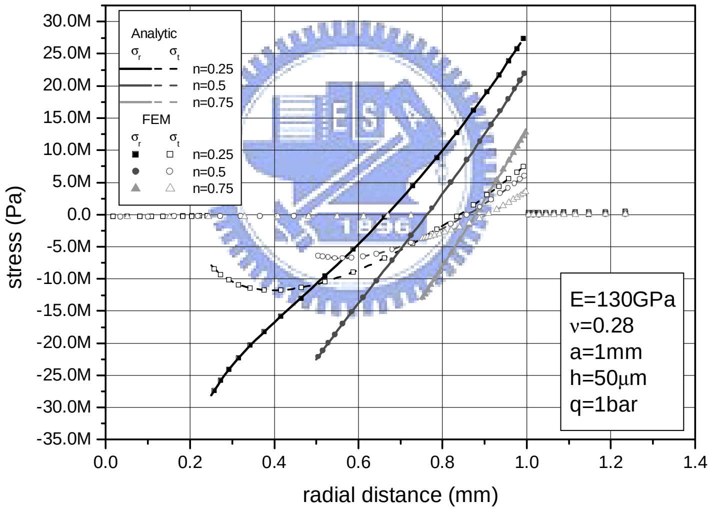

(b)

Figure 3.4. Analytic solutions of Case (A) in comparison with FEM results for: (a) the distribution of the deflection and (b) longitudinal and transverse stresses along the radial distance with respective to different ratios, n**.**

Attention should be paid on Eq. (3.9), since it contains the information about the design of a CBPS. As we can see, the longitudinal stress is a fourth order function of r. Even the magnitudes of the stresses at the inner and outer edge of the membrane are the same, but the distribution of the stress is nonlinear along the radius. Moreover, the position, where σ_r is zero, is not at the middle of the annular membrane. This property will cause a pair of non-balanced longitudinal stresses if the piezoresistors are not precisely situated at the inner and outer edge of the circular membrane. To see the changes of the stress resulting from a small displacement from the edge (in other words, the sensitivity of the sensor due to the misplacement of the piezoresistors), the slopes of the stresses at the outer and inner membrane are

$$\sigma_{r1}'(1) = \frac{3}{4}\frac{qa}{h^2}[(1-\nu)n^2 + (3+\nu)] \tag{3.29}$$

and

$$\sigma_{r1}'(n) = \frac{3}{4}\frac{qa}{h^2}[(1-\nu)n^{-1} + (3+\nu)n], \tag{3.30}$$

respectively. As n approaches 1, the slope of these two stresses becomes the same. Thus, the distribution of the longitudinal stress along the radius becomes linear and the zero stress will be in the middle of the annular membrane. However, as the radius of the center boss becomes larger, the longitudinal stress will become smaller. When the longitudinal stress is smaller than the maximum transverse stress of the CMPS, the CBPS has no more advantage over the high sensitivity. Therefore, a criterion to limit

n is derived:

$$\frac{3qa^2}{8h^2}(1+\nu) < \frac{3qa^2}{4h^2}(1-n^2), \quad n > 0 \tag{3.31}$$

The ratio n should satisfy the following inequality,

$$0 < n < \sqrt{\frac{1-\nu}{2}} \tag{3.32}$$

in order to achieve a higher sensitivity for the CBPS. The curve of this inequality is illustrated in Fig. 3.5 with a distribution of Poisson's ratio from 0 to 0.5. This range of Poisson's ratio is chosen for the application of most materials. As we can see in this figure, a choice of $n < 0.5$ yields a highly sensitive CBPS with all kinds of materials.

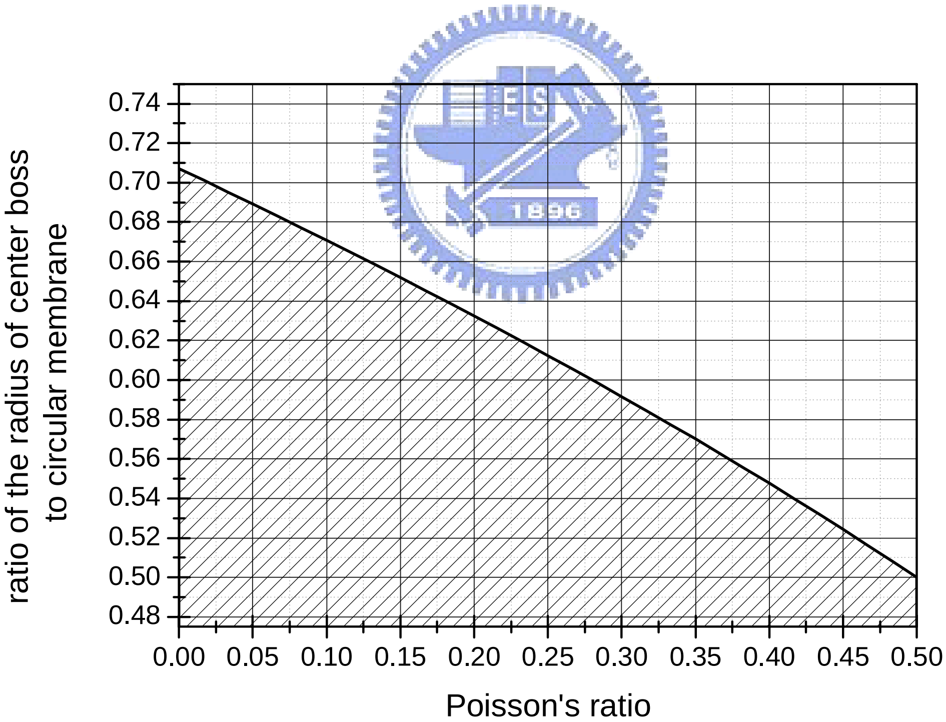

Figure 3.5. Determination of the ratio of the radius of center boss to the radius of circular membrane at a given Poisson's ratio.

Fig. 3.6 shows the distribution of the deflection and the stresses in Case (B) when n is 0.25, 0.5 and 0.75, respectively. In comparison to Case (A), the stresses are evidently smaller and do not have the same magnitude with opposite numeric signs at the edge of the annular structure.

Fig. 3.7 shows the dependence of these stresses on the ratio n. Both Case (A) and (B) are drawn together, so the longitudinal stresses at 1 bar can be compared. As we can see, when the ratio n is smaller than 0.13, the longitudinal stress at the inner edge is larger than the one of Case (A) at the same applied pressure because the stress is concentrated at the edge of the center boss as it is getting smaller.

If this structure is used as a pressure sensor and the piezoresistors are placed at the outer and inner edge of the membrane as in Case (A), the sensitivity of the sensor is

$$S_2 = \pi_r \frac{3qa^2}{8h^2} \frac{(1-n^2)(2(1-n^2)^2 + (1-n^4)\ln n - 4n^2 \ln^2 n)}{(1-n^2)^2 - 4n^2 \ln^2 n} \qquad (3.33)$$

To compare the sensitivities of Case (A) and (B), Fig. 3.8 is drawn with a Gauge Factor (GF) of 30. As we can see, the sign of the sensitivity in Case (B) is negative since the longitudinal stress at the outer edge of the membrane is smaller than at the inner edge. Moreover, the sensitivity goes down sharply as n approaches 0 because the longitudinal stress at the inner edge increases sharply as we have seen in Fig. 3.7.

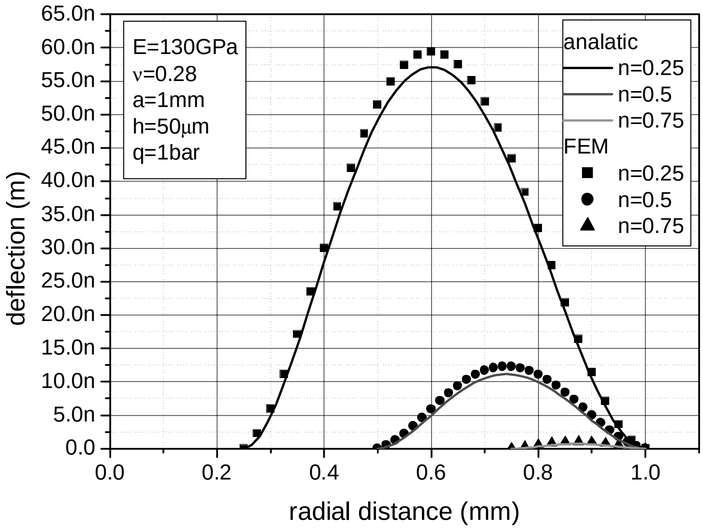

(a)

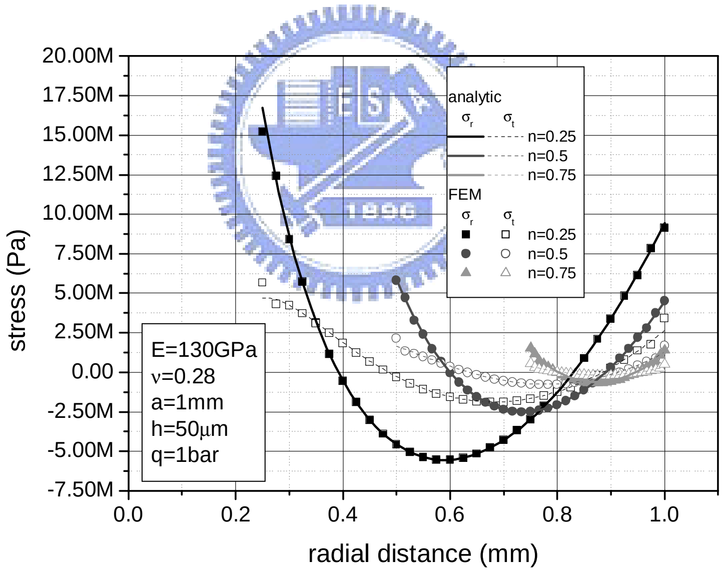

(b)

Figure 3.6. Analytic solutions of Case (B) in comparison with FEM results for (a) the distribution of the deflection and (b) longitudinal and transverse stresses along the radial distance with respect to different ratios, n.

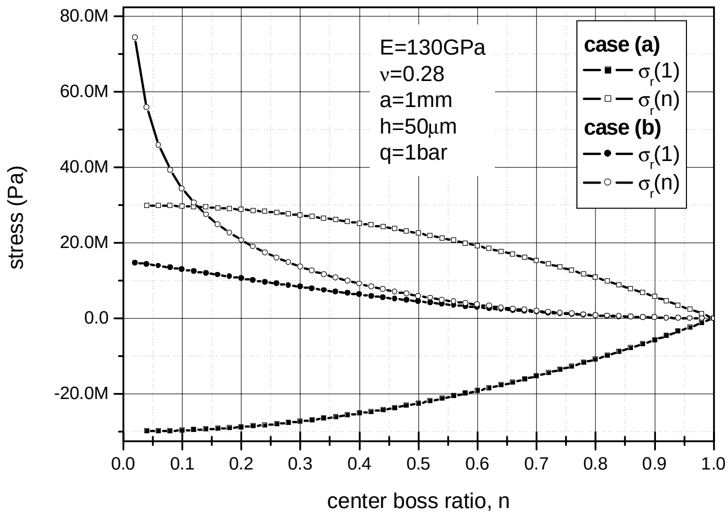

Figure 3.7. Longitudinal stresses with respect to the ratio of the radius of the center boss to the radius of the circular membrane.

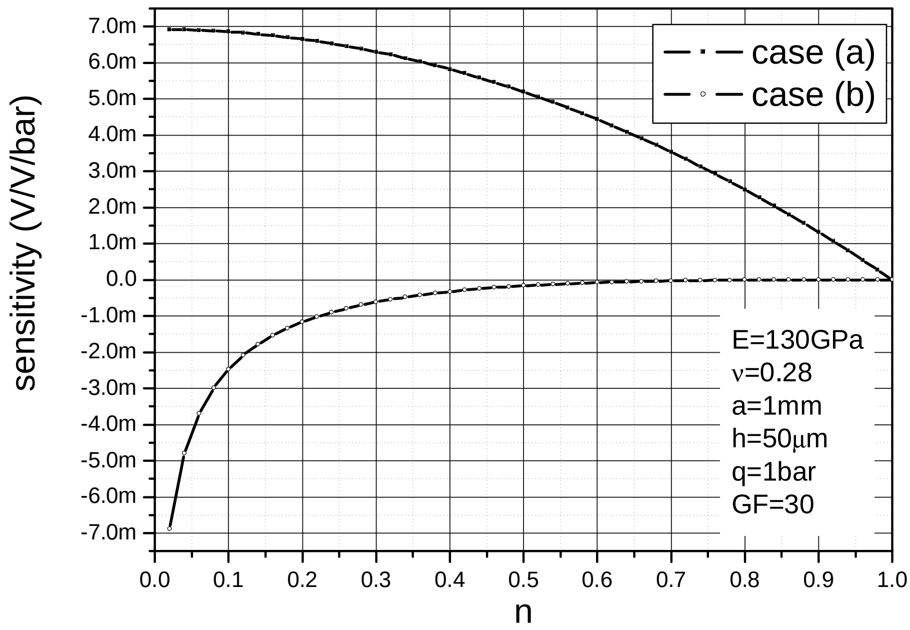

Figure 3.8. Sensitivity of Case (A) and Case (B) with respect to n.

Fig. 3.9 is drawn in order to examine Case (C). The distribution of the deflection and stresses of a CBPS is shown in that figure when the applied pressure is larger than the threshold pressure. In this case, the threshold pressure is set to 10 bar. According to Table 3.1, it will cause about 6.9 μm deflection of the membrane. Therefore, d is set to this value. Since n is 0.25, the change of the stresses is larger when the applied pressure is smaller than the threshold pressure which is coincident to Fig. 3.7.

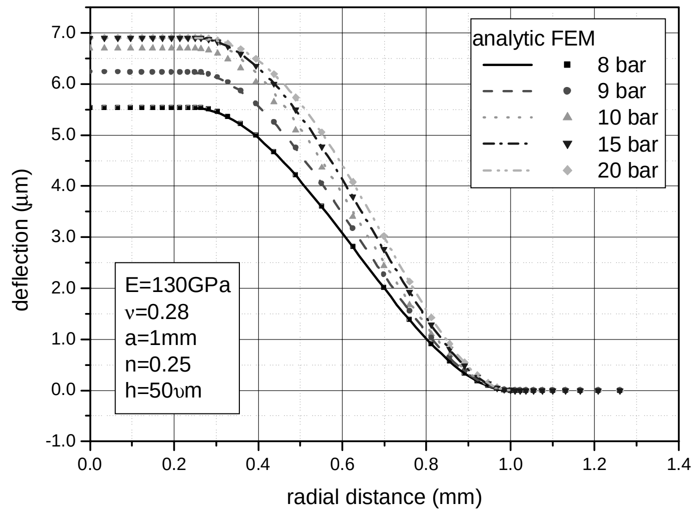
analytic FEM
8 bar
9 bar
10 bar
15 bar
20 bar
E=130GPa
ν=0.28
a=1mm
n=0.25
h=50υm
deflection (μm)
radial distance (mm)

(a)

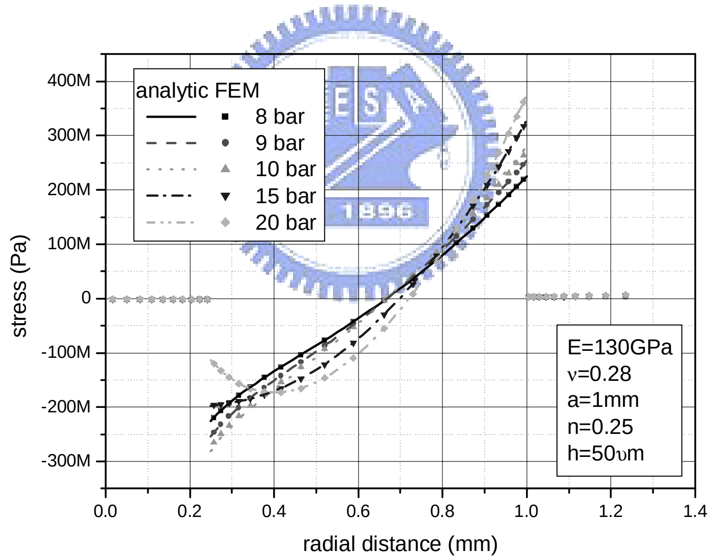
analytic FEM
8 bar
9 bar
10 bar
15 bar
20 bar
E=130GPa
ν=0.28
a=1mm
n=0.25
h=50υm
stress (Pa)
radial distance (mm)

(b)

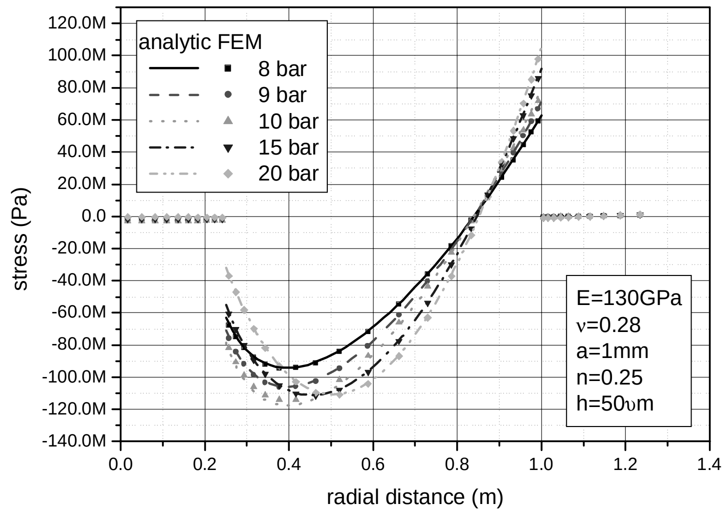

(c)

Figure 3.9. Analytic solutions of Case (C) in comparison with FEM results for: (a) the distribution of the deflection, (b) longitudinal and (c) transverse stresses along the radial distance with respect to different pressures.

3.2 Design of Piezoresistive Tactile Sensors Based on Circular Membrane with Center Boss Structure

3.2.1 Introduction

When a robotic hand tries to grasp an object, sensors are needed to help the hand to determine the magnitude, the position and the direction of the force or the torque it applies on the object. Only then can the robotic hand take the object stable and safely.

The so-called fingertip sensors are used to accomplish these tasks. Fingertip sensors have been categorized into intrinsic force/torque sensors and extrinsic tactile sensor [42][43]. Unlike the intrinsic force/torque sensor, which detects more than one degree of the force and torque at one device, the extrinsic tactile sensor detects the contact force only at a single point and in normal direction. By collecting data of many extrinsic tactile sensors in a 2-dimensional space, the tactile sensor array is formed and thus, a force image of the contacted object can be obtained. In recent years, many tactile sensors were proposed based on different materials, structures and fabrication methods[44-50]. Despite their good performance, none of them dominates the market, due to the costs[51] caused by either using a special material to sense the force or a complex packages to introduce the force to the sensor. These problems were solved by introducing a MEMS (Micro Electro-Mechanical System) based piezoresistive pressure sensor[52], which can be used as a piezoresistive tactile sensor[53-56], therefore becoming the most successful product for this application. Having the same advantages as piezoresistive pressure sensors, piezoresistive tactile sensors provide high sensitivity, good linearity, low hysteresis, an easy sensing circuit and the possibility of batch processing. However, those proposed tactile sensors still require additional packaging to introduce the force to the sensor because there is no force-conducting structure on the membrane. Moreover, in these previous researches, the distribution of the stress in the membrane of the sensor has not been analyzed in detail when a contact “force” instead of a “pressure” is applied to the sensor since the behavior of a force on a sensor is different from a pressure on a sensor. Therefore, a piezoresistive tactile sensor with a circular membrane and a center boss is proposed and analyzed in order to give a design concept. It is known that a piezoresistive pressure sensor with a circular membrane and center boss has higher sensitivity and better linearity than one without center boss[57]. Moreover, the center boss on the membrane can provide a structure to conduct force and thus, could reduce the complexity of manufacturing and the costs.

3.2.2 Analysis

The proposed tactile sensor is illustrated in Fig. 3.10. It contains 3 parts: a center boss which serves as a force-conducting structure, a circular membrane which serves as a force-sensing structure and a frame which is used to support the center boss and the circular membrane. When a force is applied to the sensor, the force-conducting structure introduces the applied force to the sensing structure. The sensing elements on the sensing structure, which are piezoresistors in Fig. 3.10, convert mechanical signals to electrical signals. Therefore, the contact force can be obtained through a calibration process. In our design, a center boss that is a little higher than the surrounding frame is used to conduct the applied force. This structure will limit the movement of the contacting object as illustrated in Fig. 3.11. If the deflection of the membrane is larger than the distance between the sensor and the bottom plate, which may be a glass or a ceramic, the plate will also constrain the further movement of the sensor and, therefore, avoid the further deflection of the circular membrane. As a result, the sensor will not be destroyed if an over-range contact force occurs. This distance can be determined once the deflection function of the membrane is known.

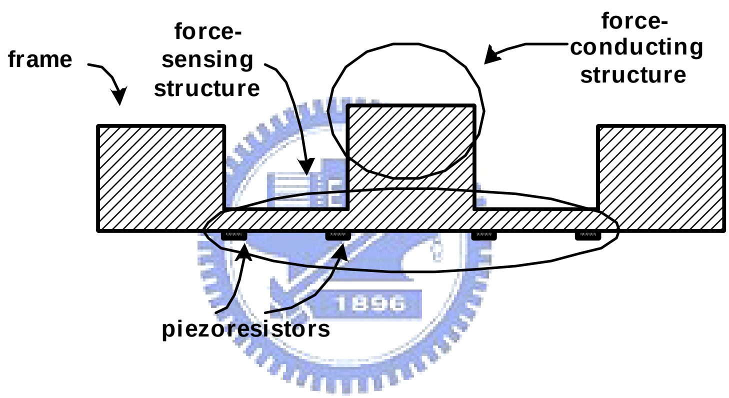

Figure 3.10. Cross section view of the proposed tactile sensor.

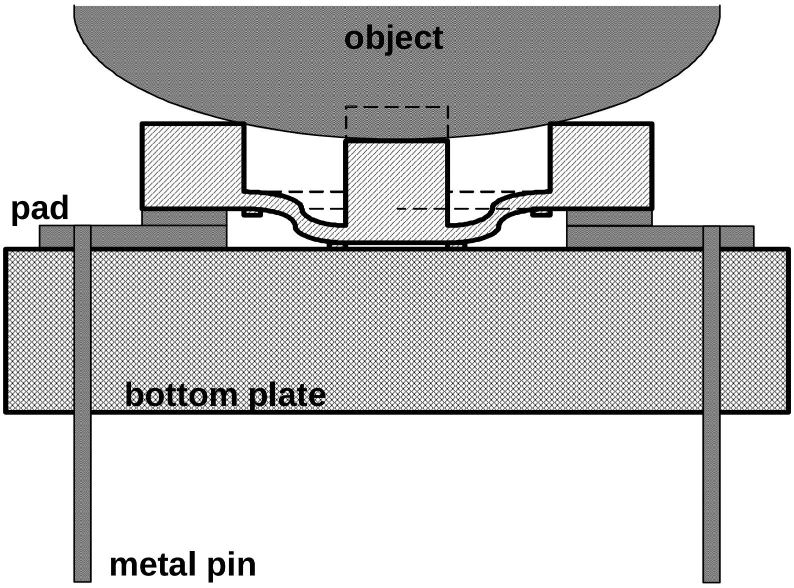

Figure 3.11. Deflection of the tactile sensor while an object contacts.

Because the tactile sensor is based on a circular membrane with center boss structure, the differential function based on symmetrical bending of circular plates will be used to derive the solution. First, the distribution function of the deflection of the circular membrane with center boss structure due to the contact force will be derived. Then, this function will be used to obtain the distribution function of the longitudinal and transverse stress. After obtaining these stress functions, the sensitivity of the tactile sensor with a specified geometry can be evaluated.

The model of the tactile sensor is illustrated in Fig. 3.12. The circular membrane has a radius a and a thickness h and the center boss has a radius b. The deflection, $w(r)$, of a circular membrane along the radial distance r due to a shear force Q, which is defined by per unit length of the cylindrical section of radius r, can be expressed as

$$\frac{d}{dr}\left[\frac{1}{r}\frac{d}{dr}\left(r\frac{dw}{dr}\right)\right]=\frac{Q}{D}, \tag{3.34}$$

where D is the flexural rigidity of the plate and is equal to

$$D=\frac{Eh^3}{12(1-\nu^2)}, \tag{3.35}$$

where E is the Young's modulus and ν is Poisson's ratio.

As a contact force P is applied to the center boss of the tactile sensor, the shear force per unit length of a circumference with a radius r can be expressed as

$$Q=\frac{P}{2\pi r}. \tag{3.36}$$

Substituting this equation in Eq. (3.34) and integrating, we can obtain the following expression:

$$w(r)=P\frac{r^2}{8\pi D}\left(\ln\frac{r}{a}-1\right)-\frac{C_1 r^2}{4}-C_2\ln\frac{r}{a}+C_3. \tag{3.37}$$

The three constants in Eq. (3.37) will be further determined by three boundary conditions. We assume that there is no deflection at the outer edge of the membrane and the slopes of the deflection are zero at both the outer and inner edge:

$$w(a)=0,\quad w'(a)=0 \quad \text{and} \quad w'(b)=0.$$

So the deflection of the membrane can be solved and expressed as

$$w(r)=\frac{Pa^2}{16\pi D\left(1-(b/a)^2\right)}\left\{-2(\frac{b}{a})^2\ln\frac{b}{a}\left[1-(\frac{r}{a})^2+2\ln(\frac{r}{a})\right]+(1-(\frac{b}{a})^2)\left[1-(\frac{r}{a})^2+2(\frac{r}{a})^2\ln\frac{r}{a}\right]\right\}$$

(3.38)

After a normalization of this equation by substituting $b=na$ $(0<n<1)$ and $r=xa$ $(0<x<1)$, this equation can be rewritten as

$$w(x)=\frac{Pa^2}{16\pi D(1-n^2)}\left[2n^2\ln n(-1+x^2-2\ln x)+(1-n^2)(1-x^2+2x^2\ln x)\right].$$

(3.39)

The corresponding longitudinal and transverse stress can be obtained by the following equations,

$$\sigma_r(r)=\frac{6M_r(r)}{h^2}=-\frac{6D}{h^2}\left(\frac{d^2w(r)}{dr^2}+\frac{\nu}{r}\frac{dw(r)}{dr}\right) \quad (3.40)$$

and

$$\sigma_t(r)=\frac{6M_t(r)}{h^2}=-\frac{6D}{h^2}\left(\frac{1}{r}\frac{dw(r)}{dr}+\nu\frac{d^2w(r)}{dr^2}\right). \quad (3.41)$$

Therefore, the longitudinal and transverse stress due to the applied force P can be expressed as

$$\sigma_r(x)=\frac{3P}{2\pi h^2}\left[-1-(1+\nu)\frac{n^2}{1-n^2}\ln n-(1-\nu)\frac{n^2}{1-n^2}\ln n\frac{1}{x^2}-(1+\nu)\ln x\right]$$

(3.42)

and

$$\sigma_t(x) = \frac{3P}{2\pi h^2}\left[-\nu - (1+\nu)\frac{n^2}{1-n^2}\ln n + (1-\nu)\frac{n^2}{1-n^2}\ln n\frac{1}{x^2} - (1+\nu)\ln x\right] \tag{3.43}$$

As we can see from Eqs. (3.42) and (3.43), the distributions of the stresses depend only on the thickness of the membrane and the aspect ratio of the inner to outer radius of the annular structure.

The solutions at the inner and outer edge of the annular structure can be obtained by substituting x with n and 1 in Eqs. (3.39), (3.42) and (3.43).

$$w(n) = \frac{Pa^2}{16\pi D}\frac{(1-n^2)^2 - 4n^2(\ln n)^2}{1-n^2} \tag{3.44}$$

$$\sigma_r(n) = -\frac{3P}{2\pi h^2}\frac{1-n^2+2\ln n}{1-n^2} \tag{3.45}$$

$$\sigma_r(1) = -\frac{3P}{2\pi h^2}\frac{1-n^2+2n^2\ln n}{1-n^2} \tag{3.46}$$

$$\sigma_t(n) = -\frac{3P\nu}{2\pi h^2}\frac{1-n^2+2\ln n}{1-n^2} \tag{3.47}$$

$$\sigma_t(1) = -\frac{3P\nu}{2\pi h^2}\frac{1-n^2+2n^2\ln n}{1-n^2} \tag{3.48}$$

Eq. (3.44) describes the maximum deflection of the sensor when a contact force is applied. The maximum force that can be applied to the sensor is reached when the maximum stress of the membrane exceed the yield stress, σ_{ys} of the sensor's material. Therefore, from Eq. (3.45), the magnitude of the maximum applicable force is

$$P_{\max} = -\frac{2\pi h^2\sigma_{ys}}{3}\frac{1-n^2+2\ln n}{1-n^2}. \tag{3.49}$$

Substituting this equation in Eq. (3.44), the maximum deflection due to this force is

$$w_{\max} = -\frac{a^2 h^2 \sigma_{ys}}{24D} \frac{(1-n^2)^2 - 4n^2 (\ln n)^2}{1 - n^2 + 2 \ln n}. \tag{3.50}$$

This deflection is used to determine the height between the center boss and the supporting frame of the sensor and also the distance between the center boss and the bottom plate to form an over-range protection.

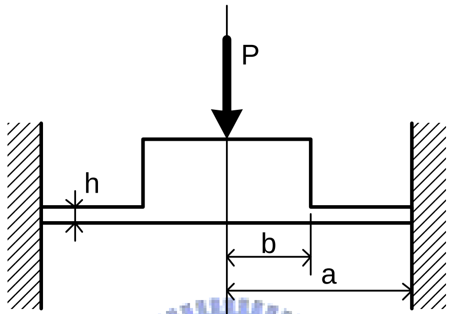

(a)

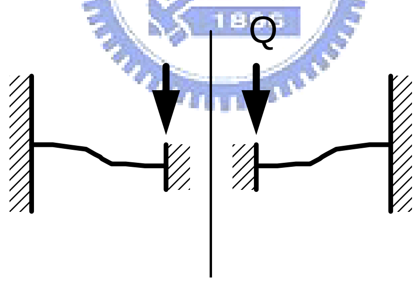

(b)

Figure 3.12. Model of the proposed tactile sensor (a) a circular membrane with center boss structure when the force, P, is applied to the center (b) an annular structure with the fixed inner and outer edge when the shear force, Q, is distributed along the inner edge uniformly.

From Eqs. (3.45), (3.46) and Eqs. (3.47), (3.48), we can find that the longitudinal stress is larger than the transverse stress since the transverse stress has the same magnitude but is smaller by a factor of ν. In order to obtain a tactile sensor with a high sensitivity, the longitudinal piezoresistive effect is taken into consideration. However, as we can see from Eqs. (3.45) and (3.46), the magnitudes of the longitudinal stresses at the inner and outer edges are not the same as for the CBPS.

3.2.3 Simulation and Discussion

According to the equations derived above, some numeric figures are presented to illustrate the performance of the sensor. The tactile sensor in the following simulation has the same geometry as the CBPS: The thickness is 50 μm and the radius of the membrane is 1 mm. A Young's modulus of 130 GPa and a Poisson ratio of 0.28 of (100) single crystal silicon is used. Fig. 3.13 shows the typical distribution of the deflection and the stresses of a silicon-based tactile sensor along the radial distance, with n equals 0.25, 0.5 and 0.75, respectively. First of all, we can find that the magnitudes of the deflection and the stresses decrease as n becomes larger. Secondly, the longitudinal stress is larger than the transverse one. Therefore, the longitudinal piezoresistive effect is preferred in the design of the sensor. Thirdly, the magnitudes of the stresses at the inner and outer edge of the annular structure are not the same. But we can find a pair of longitudinal stresses that have the same magnitudes with opposite numerical signs on the annular membrane according to Eq.(3.42) by a numerical method in order to design a balanced full Wheatstone bridge. But a significant loss of sensitivity results when using this setup. In a different advance, we consider the case when the piezoresistors are placed at the inner and outer edge of the annular membrane and examine if the linearity will be degraded.

Fig. 3.14 illustrates the longitudinal and transverse stress at the inner and outer edge as a function of n. As we can see, the longitudinal stress at the inner edge is larger than the other components. When n approaches 1, the magnitude of the stresses at the inner and the outer edge will approach the same value but the corresponding longitudinal stress decreases significantly. Especially when n is smaller than 0.1, the longitudinal stress increases dramatically because the component $\ln n$ in Eq. (3.45) begins to govern.

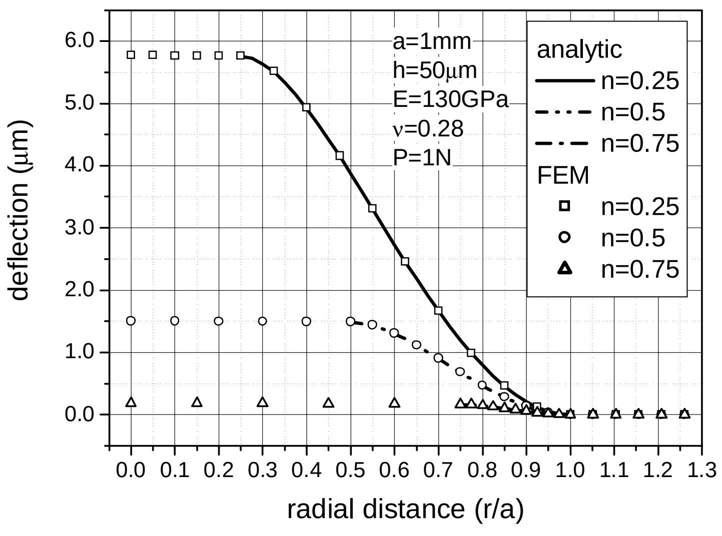
a=1mm
h=50μm
E=130GPa
ν=0.28
P=1N
analytic
n=0.25
n=0.5
n=0.75
FEM
n=0.25
n=0.5
n=0.75
deflection (μm)
radial distance (r/a)

(a)

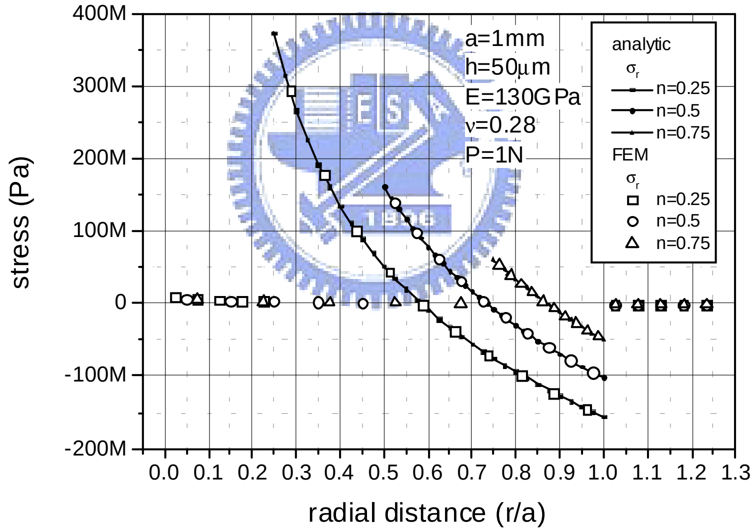
a=1mm
h=50μm
E=130GPa
ν=0.28
P=1N
analytic
σr
n=0.25
n=0.5
n=0.75
FEM
σr
n=0.25
n=0.5
n=0.75
stress (Pa)
radial distance (r/a)

(b)

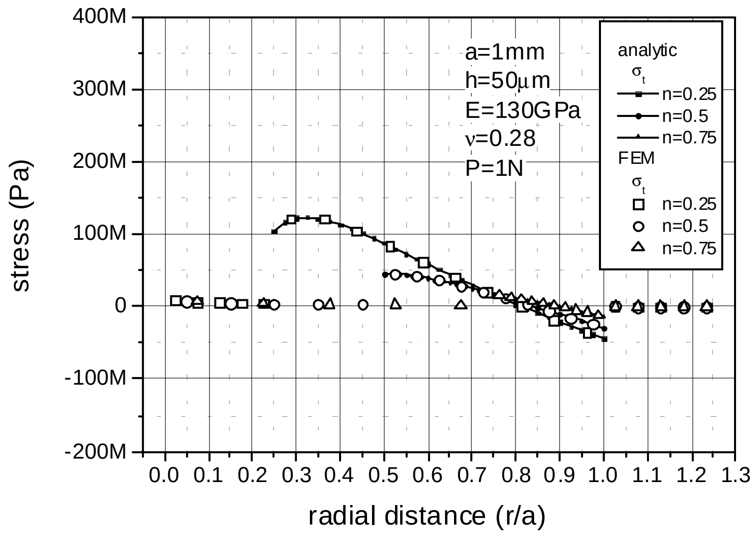

(c)

Figure 3.13. Distribution of (a) the deflection and (b) longitudinal and (c) transverse stress with different n.

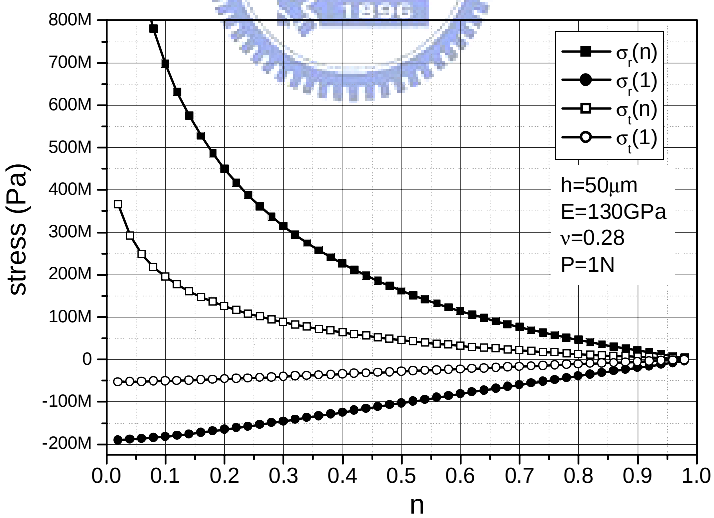

Figure 3.14. Longitudinal and transverse stresses at the inner and outer edge of the annular structure with respect to n.

The arrangement of the piezoresistors on the tactile sensor is the same as on the CBPS as illustrated in Fig. 3.2. The piezoresistors, the applied voltage and current are all situated along the radial direction so only the longitudinal piezoresistive effect will be considered. If the change in resistance ΔR, between the inner and outer edge of the annular structure is assumed as a factor d, the sensitivity of the tactile sensor based on a Wheatstone bridge can be expressed as

$$\frac{\Delta V}{V}=\frac{(1+d)\dfrac{\Delta R}{2R}}{1+(1-d)\dfrac{\Delta R}{2R}}=\frac{(1+\dfrac{\sigma_r(1)}{\sigma_r(n)})\dfrac{\pi_r\sigma_r(n)}{2}}{1+(1-\dfrac{\sigma_r(1)}{\sigma_r(n)})\dfrac{\pi_r\sigma_r(n)}{2}}. \tag{3.51}$$

As we can see from the above equation, the term, $1-\sigma_r(1)/\sigma_r(n)$, in the denominator will result in a nonlinearity of the output signal. But if we consider the piezoresistive effect of silicon, the term $\pi_r\sigma_r(n)$ is 3 orders smaller than 1. Therefore, the denominator in Eq. (3.51) can be approximated as 1. As a result, the above equation can be further expressed as

$$\frac{\Delta V}{V}\sim\frac{(1+\sigma_r(1)/\sigma_r(n))}{2}\pi_r\sigma_r(n), \tag{3.52}$$

which has a linear relationship between the output voltage and input stress . Thus, even though a non-balance Wheatstone bridge is used in the proposed tactile sensor, a high sensitivity with little loss of linearity can be obtained.

Usually, the gauge factor instead of the piezoresistance coefficient is used to design piezoresistive sensors. With the introduction of the longitudinal gauge factor,

K_r, and the longitudinal strain, ε_r, Eq. (3.52) can be rewritten as

$$\frac{\Delta V}{V} \sim \frac{(1+\varepsilon_r(1)/\varepsilon_r(n))}{2} K_r \varepsilon_r . \qquad (3.53)$$

An FEM as described before is used to verify these analytic solutions. An element of an axis-symmetric structural shell, SHELL51, is used for simple and efficient computing. The geometry of the sensor is the same as the one used in the analytic solution. The thickness of the center boss is 525 μm. The simulated results are accompanied with the analytic solution in Fig. 3.13 and agree with the derived analytic solutions.